Orientation Angle Distributions of Drops after an 80-m Fall Using a 2D Video Disdrometer

GWO-JONG HUANG, V. N. BRINGI, AND M. THURAI

Colorado State University, Fort Collins, Colorado

(Manuscript received 2 October 2007, in final form 22 January 2008)

ABSTRACT

This note reports on the use of a 2D video disdrometer to estimate the orientation of drops (>2 mm) that were generated artificially and allowed to fall 80 m from a bridge with no obstruction and under calm conditions. This experimental setup enabled a large number of drops to be generated, up to 10 mm in horizontal dimension.

The distribution of the canting angles for all drops >2 mm was found to be nearly symmetric about 0° with standard deviation between 7° and 8°. From the canting angle distributions derived from the two orthogonal camera view planes, the distributions of the polar (θ) and azimuth (ϕ) angles were deduced; these two angles describe the 2D orientation of the symmetry axis. The azimuthal angle distribution was found to be nearly uniform in the range $(0, 2\pi)$, whereas the distribution of $p_\Omega(\theta) = p(\theta)\sin\theta$ was similar in shape to a special form of the Fisher distribution that is valid for describing the statistics on a spherical surface. The standard deviation of $p_\Omega(\theta)$ showed that larger drops are more stably oriented than smaller ones. This is in agreement with previous radar-based results of standard deviation of the canting angle decreasing with increasing Z_{dr}.

1. Introduction

Inferences made from circularly polarized radar measurements have shown that raindrops form a highly oriented medium with their symmetry (minor) axis close to vertical (McCormick et al. 1972). Later, definitive X-band measurements using rotating linear polarizations in heavy rain by Hendry et al. (1987) showed that the mean canting angle $\overline{\beta}$ was nearly 0°, with the standard deviation σ_β close to 6°. The canting angle is the angle between the projection of the drop's symmetry axis on the polarization plane and the projection of the "true" local vertical direction on this same plane.

Theoretical studies by Beard and Jameson (1983), based on raindrop response to shear produced by homogeneous isotropic turbulence, predicted that the mean canting angle should be close to 0° with a standard deviation $\sigma_\beta < 4°$ for turbulent intensities <0.2 $m^2\,s^{-3}$. They actually found that $\tan(\beta)$ was Gaussian; however, for small β, $\tan(\beta) \approx \beta$ and the Gaussian shape also applies to β. Their model predictions are valid above the surface layer and are consistent with the radar observations of Hendry et al. (1987).

Since the work by Hendry et al. (1987) there have been few radar-based estimates of the σ_β in rain; notable are the S-band radar inferences of Ryzhkov et al. (2002), who derived a simple formula for σ_β based on Z_{dr} and LDR data, whereas Huang et al. (2001, 2003) used a variant of the Hendry et al. (1987) approach but with the full covariance matrix data to infer σ_β. These latter studies showed that σ_β could be in the range of 5° to 15°. On average, a systematic decrease in σ_β with increasing equivolume spherical diameter D_{eq} was also noted, and it was inferred that large drops were more stably oriented than small drops.

Polarimetric radar-based algorithms for estimating rain rate or parameters of the drop size distribution generally assume either perfect orientation of the drop symmetry axis ($\beta = 0°$) or a Gaussian distribution with $\overline{\beta} = 0°$ and σ_β varying between 5° and 10° [e.g., chapter

Corresponding author address: V. N. Bringi, Dept. of ECE, Colorado State University, Fort Collins, CO 80523-1373.
E-mail: bringi@engr.colostate.edu

DOI: 10.1175/2008JTECHA1075.1

7 of Bringi and Chandrasekar (2001) and references therein]. The former model gives a linear depolarization ratio (LDR) of zero, whereas the latter gives finite values and hence is more realistic. The dependence of LDR on σ_β is approximately proportional to $[1 - \exp(-8\sigma_\beta^2)]$; for $K_{\rm dp}$ it is $\exp(-2\sigma_\beta^2)$. Calculations show that the dependence of $Z_{\rm dr}$ on σ_β is generally small for $\sigma_\beta < 10^\circ$ (a few tenths of a decibel; see Fig. 3.18 of Bringi and Chandrasekar 2001). From a radar-based algorithm development viewpoint, it would be useful to have direct measurements of $\bar{\beta}$ and σ_β for raindrops, which is possible with a 2D video disdrometer (2DVD; Schönhuber et al. 2007; Randeu et al. 2002; Kruger and Krajewski 2002).

The 2D video disdrometer has two orthogonally placed line scan cameras, which give two views of the raindrop as it passes through the sensor area. Here, the term "canting angle" is used (even though it is defined for radar applications) because each camera view can be thought of as being in the "polarization" plane of a radar beam at a zero elevation angle. As such, two canting angles are derived for each drop (the angle being defined from the vertical line that is perpendicular to the light planes). Schöenhuber et al. (2000) showed that the instrument was sensitive enough to detect $\beta > 0.5^\circ$ by artificially tilting the light planes and noting a corresponding shift in the mean β. They also reported on the estimation of β for artificial drops after a fall distance of 35 m, as well as in natural rain. Here we continue their studies, using artificially generated drops (up to 10 mm) that were allowed to fall a distance of 80 m before entering the sensor area. At this fall distance, it is expected that the drops will have attained a "steady" orientation state from which reliable canting angle distributions in two orthogonal planes may be estimated. In addition, the true orientation of the symmetry axis can be determined, that is, the polar (or zenith) angle (θ) from the vertical direction and the azimuthal angle (ϕ).

To further clarify the above, we distinguish between the distribution of the canting angle (β) versus the distribution of the orientation of the symmetry axis with respect to the true local vertical direction. By *orientation* we mean the direction of the symmetry axis as described by polar angle (θ) and the azimuth angle (ϕ) defined with respect to the local XYZ system, with the Z axis directed along the vertical direction. In general, a third angle is needed for particles which are not rotationally symmetric, but here we assume that rain drops are bodies of revolution (e.g., oblate). The orientation distribution should be properly described by the probability that the symmetry axis lies between the solid angle Ω to $\Omega + d\Omega$ on a spherical surface, which (assuming that θ and ϕ are independent) can be written as $p_\Omega(\theta, \phi) = p(\theta) \sin\theta\, p(\phi)$. There is no theoretical reason to believe (but yet to be experimentally verified) that the distribution of ϕ is other than uniform between $[0, 2\pi]$ and independent of θ, in which case $p_\Omega(\theta, \phi) = (1/2\pi)\, p_\Omega(\theta)$. The probability distribution function (pdf), $p_\Omega(\theta)$, is a special case of the general Fisher distribution valid for describing statistics on a spherical surface (Mardia 1972); it is given by

$$p_\Omega(\theta) = \frac{\kappa e^{\kappa \cos\theta}}{4\pi \sinh(\kappa)} \sin\theta, \tag{1}$$

where κ is a parameter that controls the width of the distribution. Hubbert and Bringi (1996) derive in their appendix an approximate inverse relation between κ and the standard deviation of the Gaussian form for the pdf of $p(\theta)$. We further define $p(\theta)$ from $p_\Omega(\theta) = p(\theta) \sin\theta$ (e.g., for plots of $p_\Omega(\theta)$ for various κ values, see Fig. 2.9a of Bringi and Chandrasekar 2001). Our further objective, using the 2D video estimates of canting angles in two orthogonal planes, is to show that $p(\phi)$ is approximately uniform between $[0, 2\pi]$ and that the $p_\Omega(\theta)$ is approximately of the shape of the special form of the Fisher distribution alluded to earlier. We also show that larger drops are more stably oriented compared with smaller drops, as expected from physical reasoning and consistent with past radar measurements (Huang et al. 2001, 2003). Such diameter dependence can be used in fine tuning radar retrievals of rain rate and D_o (median volume diameter) from $K_{\rm dp}$ and $Z_{\rm dr}$ data.

2. 2D video disdrometer analyses

The 2D video disdrometer operation is well described by Kruger and Krajewski (2002) and will not be repeated here. Suffice it to mention that two orthogonally placed high-speed line scan cameras, together with two parallel high-intensity light planes (Fig. 1) spaced a precise (well calibrated) distance apart (nominally 6 mm), allow for the determination of the drop's vertical speed by two orthogonal digitized "views" from which the drop volume and equivalent spherical diameter are computed, as well as the axis ratio and an approximate determination of the drop's horizontal velocity. To our knowledge there is no other commercially available disdrometer that can measure the rain microphysics in such detail.

The data described here were acquired by allowing a stream of drops to form from an open hose placed between the slats of a railway bridge 80 m above the disdrometer (for details we refer to Thurai and Bringi

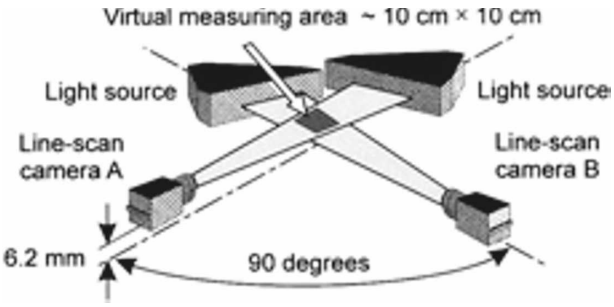

FIG. 1. Schematic illustration of the 2D video measurement principle using two light sources and two orthogonally placed fast line scan cameras. (From Kruger and Krajewski 2002.)

2005). Large drops can be formed by such a method, up to 10 mm in horizontal dimension. The 80-m fall distance is the largest reported in the literature. Prior fall distances were approximately 30 m in the laboratory (e.g., Andsager et al. 1999), and 35 m from a tower in Graz, Austria, (Schönhuber et al. 2000), but both these are believed to be insufficient for allowing larger drops to reach steady-state oscillations or orientations independent of the drop generating mechanism. In the laboratory studies the drops fall in a confined domain; in the Graz tower experiments the stream of drops was close to the tower. It is not clear if such proximity to surrounding structures could alter the drop orientation relative to the case of no obstruction at all, as in the 80-m bridge experiment.

To explain how the 2DVD is used to estimate the canting angle, we use the following example. Figure 2a shows a conical-shaped drop with no canting angle falling vertically through the two light planes. The symmetry axis (later referred to as a bisection line) is also shown. Note that a conical shape is used because large drops have a flattened base (see Thurai et al. 2007). The conical shape in Fig. 2a is based on Wang (1982):

$$x = \pm\frac{L}{\pi}\left[1 - \left(\frac{y}{c}\right)^2\right]^{1/2} \cos^{-1}\left(\frac{y}{\lambda c}\right), \qquad (2)$$

with parameters $L = 8$ mm, $c = 2$, and $\lambda = 3$. To simulate the drop falling with a finite horizontal velocity, (2) is transformed to a horizontally moving reference frame via the transformation ($x' = x + y\tan\alpha$, $y' = y$); the resulting contour is shown in Fig. 2b. Note that $\tan\alpha = U/V$, where U and V are the horizontal and vertical velocities, respectively (α is set to 25°). Figure 2b shows the bisection line, which is defined by the straight line that joins the midpoint of each scan line. The angle ζ and α are also depicted. To deskew the shape in Fig. 2b, the angle α is determined as the slope of the bisection line referenced from the vertical direction.

However, if the conical drop is canted as it enters the sensor area with a finite horizontal velocity, then it is more difficult to recover the true canting angle from the measured contour points. Figure 3a shows an initially canted cone (with canting angle = β) with no horizontal velocity. As in Fig. 2a, the symmetry axis is shown.

Now consider the case if the drop has, in addition, a finite horizontal velocity. In a horizontally moving reference frame, the transformation is $x'' = x + y\tan\alpha$, $y'' = y$, where (x, y) are the contour points in Fig. 3a. Figure 3b shows the contour based on the points (x'', y'') which would be measured by the 2DVD (the quantization error is not considered in the example). Also

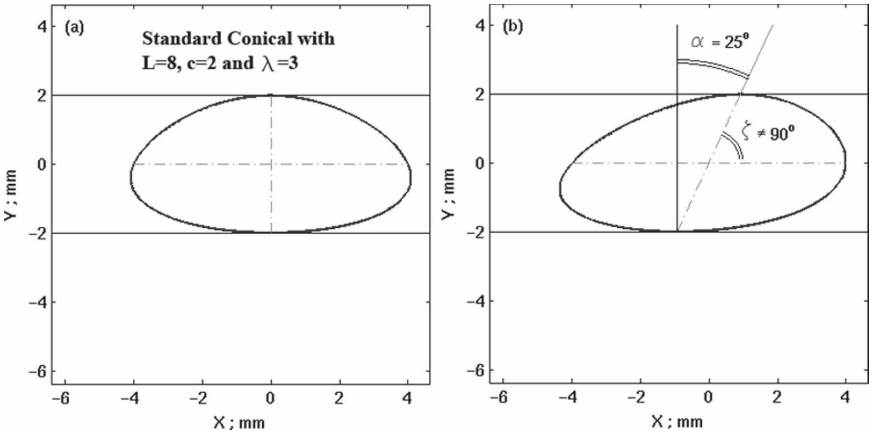

FIG. 2. Idealized representation of cases in which (a) an initially uncanted drop falls vertically (with the vertical dashed line representing the symmetry axis) and (b) the drop additionally has finite horizontal velocity. The slanted dashed line in (b) is defined as the bisection line and $\tan\alpha$ is the ratio of horizontal to vertical drop velocity. Both figures show the expected single camera view of the 2D video disdrometer without any quantization or other errors.

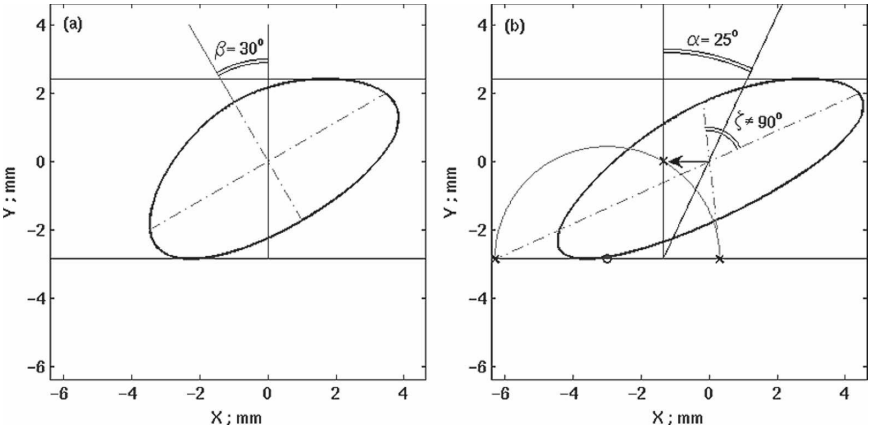

FIG. 3. (a) Same as Fig. 2a, but drop has an initial (or intrinsic) canting angle of 30°; (b) additionally, drop has finite horizontal velocity. The (close to vertical) slanted dashed line is defined as the bisection line; the semicircle is used to determine the deskewing procedure (as explained in the text).

shown are the bisection line and the angles α and ζ. The deskewing procedure (to determine the true canting angle) is now more complicated because only the contour points (x'', y'') are known a priori from the camera data. First assume that the bisection line is known (the procedure will be described below). From the bisection line, we can determine the angle α by forcing the angle $\zeta = 90°$. This is done by determining the shift required in the x'' coordinate determined as follows: a horizontal line is drawn through the center of the bisection line that intersects the semicircle at two points as illustrated in Fig. 3b. The shorter of the two distances is chosen as the Δx required to find α and force $\zeta = 90°$ (Schönhuber et al. 2000; Schauer 1998). From the deskewed contour the "intrinsic" canting angle β can be determined.

In Fig. 4, we illustrate the method of finding the bi-

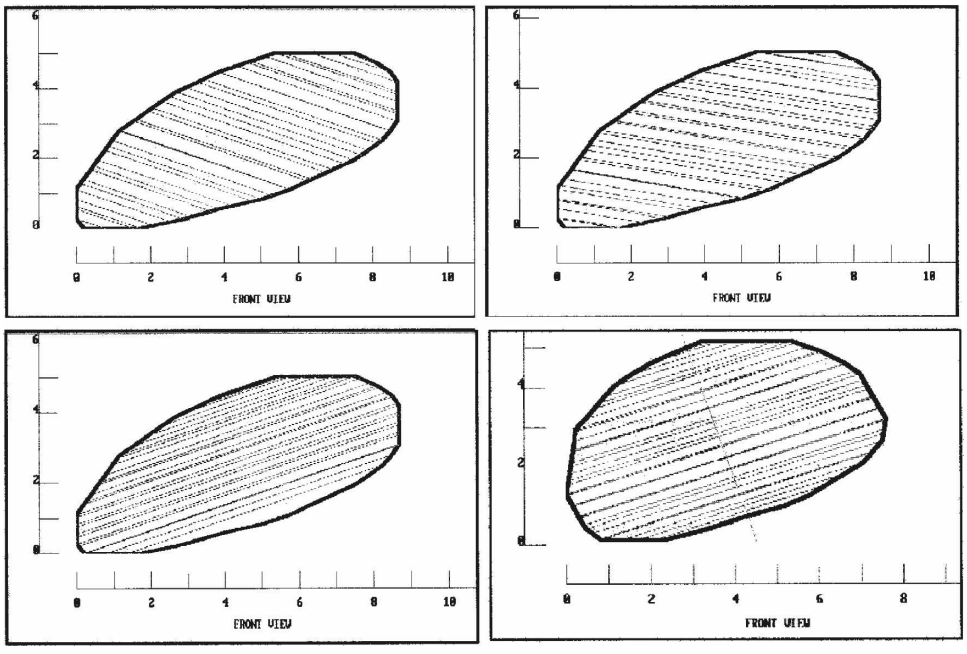

FIG. 4. The determination of the bisection line is illustrated by drawing a set of parallel lines at various angles with respect to the horizontal direction: (top left) −20°; (top right) −10°; (bottom left) + 20° (close to the true bisection line); and (bottom right) restoring the orthogonality of the bisection line and the set of parallel lines, thus determining the true drop shape and intrinsic canting angle. Axes are measured in mm. (From Schönhuber et al. 2000.)

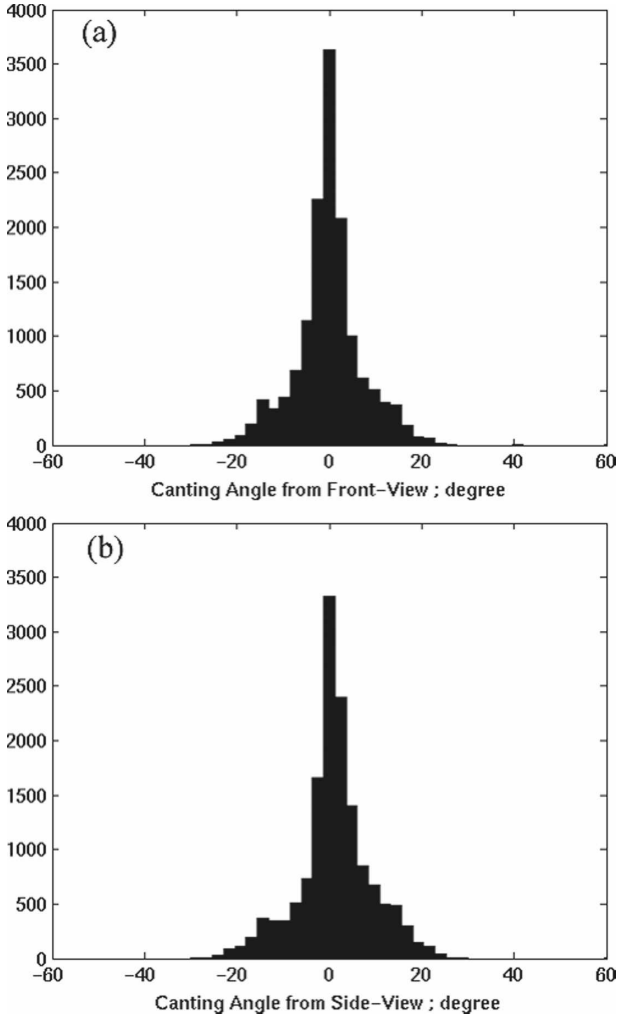

FIG. 5. Histograms of canting angles from (a) front (camera A) and (b) side (camera B) views. Note that they are almost symmetric, with a mean of 0° and std dev 7.2° and 7.8°, respectively.

section line using as an example the measured (x'', y'') contour from a single camera (Schönhuber et al. 2000). To find the bisection line, a set of parallel lines are drawn whose angle with respect to the horizontal line is changed within an interval (−50°, 50°) in steps of 0.5°. For example, Fig. 4 (top two panels and bottom left) shows the set of parallel lines oriented at −20°, −10°, and 20°, respectively. Each parallel line will intercept the contour at two points. The objective is to find the angle such that the locus of the midpoints can be fitted to a straight line with minimum rms error. Figure 4 (bottom left) shows the angle close to which the previously mentioned criteria are fulfilled. Finally, Fig. 4 (bottom right) shows the deskewed conical shape and intrinsic canting angle obtained as described in the discussion leading to Fig. 3b.

For all drops with $D_{eq} \geq 2$ mm from the 80-m fall bridge experiment (Thurai and Bringi 2005), the histograms of canting angles derived from cameras A and B are shown in Figs. 5a,b following the method described earlier. Note that the shapes of the canting angle histograms are approximately Gaussian with mean $\beta \approx 0$ and σ_β of around 7°. Because two canting angles (from cameras A and B) are measured, we can easily derive the zenith (θ) and azimuth (ϕ) angles of the drop's symmetric axis; the histogram of θ is then inferred to represent the marginal pdf of θ. The marginal pdf $p_\Omega(\theta)$ derived from the two canting angles is shown as a histogram in Fig. 6. Note that the shape is not Gaussian but instead is skewed with a mode of $\theta \approx 3°$; in essence, it approximately follows a special form of the Fisher pdf that is valid for describing the statistics on a spherical surface. The marginal pdf $p(\phi)$ is shown as a histogram in Fig. 7. Ignoring the "multimodes" that occur at regular intervals of 45° (most likely due to the algorithmic errors), the shape of the histogram suggests a uniform pdf in the range 0–2π. We note here that Metcalf (1988) assumed, for convenience and analytic tractability, a 2D Gaussian distribution on a spherical surface for the symmetry axis and showed that $\sigma_\theta \approx \sigma_\beta$ (for $\sigma_\theta \leq 15°$).

Further, for each drop class diameter interval from 2 to 7 mm (with bin width of 0.5 mm), σ_θ was calculated as a function of the midpoint of the diameter class and is shown in Fig. 8. Note how σ_θ falls with an increase in D_{eq}, the inference being that the larger drops are more stably oriented than the smaller ones. From these data σ_θ reduces from 6.8° at 2 mm to 4.8° at 7 mm. This range of values is somewhat larger than the predictions of Beard and Jameson (1983), but is consistent with those estimated from rotating linear polarizations by Hendry et al. (1987).

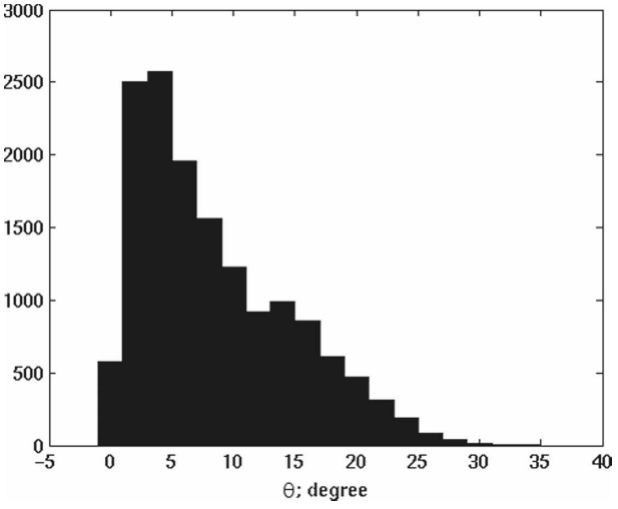

FIG. 6. Histogram of zenith angle θ derived from the two canting angle distributions in Fig. 5. It represents the marginal pdf $p_\Omega(\theta)$.

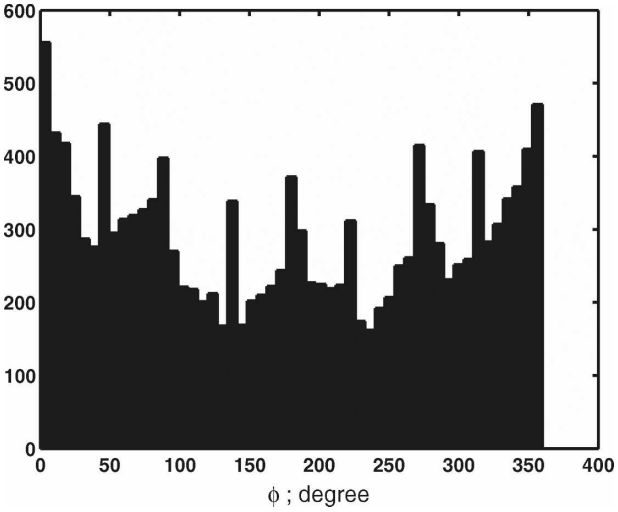

FIG. 7. Histogram of azimuth angle Φ. It is close to being uniformly distributed between $(0, 2\pi)$. The multimodes at approximately 45° spacing may be due to the algorithm used.

3. Conclusions

We have continued the earlier studies of Schönhuber et al. (2000) of using the 2D video disdrometer to estimate drop orientation angles, the drops being generated artificially and allowed to fall 80 m from a bridge with no obstruction and under calm conditions (winds <1 m s^{-1}). This setup allowed generation of very large drops (up to 10 mm in horizontal dimension) and large numbers of drops, exceeding 100 000 drops of sizes >2 mm.

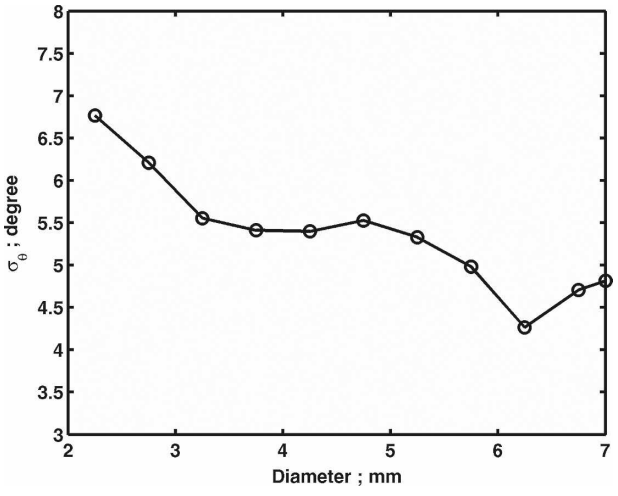

FIG. 8. Std dev of θ vs drop size D_{eq} from the 80-m fall bridge experiment. The size intervals are 2–7 mm with a 0.5-mm step. The last data point represents those drops greater than 7 mm. Note that in the calm conditions prevalent during the experiment, the large drops are more stably oriented (smaller σ_θ) than small drops (larger σ_θ).

For all drops >2 mm, the distribution of the canting angles from each camera was found to be nearly symmetric about $\beta = 0°$ with σ_β of 7°–8°. From the two canting angle distributions in the two orthogonal planes, we were able to deduce the distributions of the polar (θ) and azimuth (ϕ) angles that describe the 2D orientation of the symmetry axis. The azimuthal angle distribution was more or less uniform in the range $(0, 2\pi)$, whereas the distribution of $p_\Omega(\theta) = p(\theta)\sin\theta$ was, as expected, similar in shape to the special form of the Fisher distribution that is valid for describing the statistics on a spherical surface. The mean of the standard deviation of the histogram representing $p_\Omega(\theta)$ was shown to decrease with D_{eq}, implying that larger drops are more stably oriented than smaller ones. This is in agreement with previous radar-based results of standard deviation of the canting angle decreasing with increasing Z_{dr}. We will analyze the orientation distributions in natural rain under light wind conditions in the near future.

Acknowledgments. This work was supported by the National Science Foundation via Grant ATM-0603720. We thank Michael Schönhuber and Günter Lammer of Joanneum Research for their precise conduct of the 80-m fall bridge experiment and Prof. Walter Randeu of the Technical University of Graz for overseeing and selecting the site for the bridge experiment.

REFERENCES

Andsager, K., K. V. Beard, and N. F. Laird, 1999: Laboratory measurements of axis ratios for large raindrops. *J. Atmos. Sci.,* **56,** 2673–2683.

Beard, K. V., and A. R. Jameson, 1983: Raindrop canting. *J. Atmos. Sci.,* **40,** 448–454.

Bringi, V. N., and V. Chandrasekar, 2001: *Polarimetric Doppler Weather Radar: Principles and Applications*. Cambridge University Press, 636 pp.

Hendry, A., Y. M. M. Antar, and G. C. McCormick, 1987: On the relationship between the degree of preferred orientation in precipitation and dual-polarization radar echo characteristics. *Radio Sci.,* **22,** 37–50.

Huang, G., J. C. Hubbert, and V. N. Bringi, 2001: Precipitation canting angle distribution estimation from covariance matrix analysis of CSU-CHILL radar data. Preprints, *30th Int. Conf. on Radar Meteorology,* Munich, Germany, Amer. Meteor. Soc., 11B.6. [Available online at http://ams.confex.com/ams/pdfpapers/22111.pdf]

——, V. N. Bringi, and J. C. Hubbert, 2003: An algorithm for estimating the variance of the canting angle distribution using polarimetric covariance matrix data. Preprints, *31st Int. Conf. on Radar Meteorology,* Seattle, WA, Amer. Meteor. Soc., 8B.5. [Available online at http://ams.confex.com/ams/pdfpapers/64005.pdf]

Hubbert, J. C., and V. N. Bringi, 1996: Specular null polarization theory: Applications to radar meteorology. *IEEE Trans. Geosci. Remote Sens.,* **34,** 859–873.

Kruger, A., and W. F. Krajewski, 2002: Two-dimensional video disdrometer: A description. *J. Atmos. Oceanic Technol.,* **19,** 602–617.

Mardia, K. V., 1972: *Statistics of Directional Data*. Academic Press, 357 pp.

McCormick, G. C., A. Hendry, and B. L. Barge, 1972: The anisotropy of precipitation media. *Nature,* **238,** 214–216.

Metcalf, J. I., 1988: A new slant on the distribution and measurement of hydrometeor canting angles. *J. Atmos. Oceanic Technol.,* **5,** 571–578.

Randeu, W. L., M. Schönhuber, and G. Lammer, 2002: Real-time measurements and analyses of precipitation microstructure and dynamics. *Proc. Second European Conf. on Radar Meteorology (ERAD),* Delft, Netherlands, Copernicus Gesellschaft, 78–83.

Ryzhkov, A. V., D. S. Zrnic, J. C. Hubbert, V. N. Bringi, J. Vivekanandan, and E. A. Brandes, 2002: Polarimetric radar observations and interpretation of co-cross-polar correlation coefficients. *J. Atmos. Oceanic Technol.,* **19,** 340–354.

Schauer, G., 1998: Distrometer-based determination of precipitation parameters for wave propagation research. M.S. thesis, Technical University of Graz, 98 pp.

Schönhuber, M., W. L. Randeu, H. E. Urban, and J. P. V. Poiares Baptista, 2000: Field measurements of raindrop orientation angles. *Proc. AP2000 Millennium Conf. on Antennas and Propagation,* Davos, Switzerland, IEE, CD-ROM.

——, G. Lammer, and W. L. Randeu, 2007: One decade of imaging precipitation measurements by 2D video disdrometer. *Adv. Geosci.,* **10,** 85–90.

Thurai, M., and V. N. Bringi, 2005: Drop axis ratios from 2D video disdrometer. *J. Atmos. Oceanic Technol.,* **22,** 966–978.

——, G. J. Huang, V. N. Bringi, W. L. Randeu, and M. Schönhuber, 2007: Drop shapes, model comparisons, and calculations of polarimetric radar parameters in rain. *J. Atmos. Oceanic Technol.,* **24,** 1019–1032.

Wang, P. K., 1982: Mathematical description of the shape of conical hydrometeors. *J. Atmos. Sci.,* **39,** 2615–2622.